ORIENTAL JOURNAL OF CHEMISTRY
An International Open Access, Peer Reviewed Research Journal
www.orientjchem.org
ISSN: 0970-020 X
CODEN: OJCHEG
2025, Vol. 41, No.(2):
Pg. 654-664

Synthesis, Characterization, DFT and Molecular Docking Analysis of N-phenyl-2-((4-(3-phenylthioureido)phenyl)selanyl)acetamide

HUSSEIN BA-GHAZAL[1], TAREK A. YOUSEF[2], RAMY A. BEDIER[3], AHMED S. M. AL-JANABI[4]*, MOHAMED ALAASAR[5], OMAR K. AL DUAIJ[2] and SAAD SHAABAN[1]**

[1]Department of Chemistry, College of Science, King Faisal University, Al-Ahsa-31982, Saudi Arabia.
[2]Department of Chemistry, College of Science, Imam Mohammad Ibn Saud Islamic University (IMSIU), Riyadh-11623, Riyadh.
[3]Suez Canal Authority, Ismailia, Egypt.
[4]Department of Chemistry, College of Science, Tikrit University, Tikrit, Iraq.
[5]Faculty of Natural, Science II, Institute of Chemistry, Martin-Luther University, 06120 Halle Saale, Germany.
*Corresponding authors E-mail: dr.ahmed.chem@tu.edu.iq, sibrahim@kfu.edu.sa

http://dx.doi.org/10.13005/ojc/410235

(Received: March 05, 2025; Accepted: April 06, 2025)

ABSTRACT

In this study, we disclose the synthesis of a new organoselenium (OSe) candidate, N-phenyl-2-((4-(3-phenylthioureido)phenyl)selanyl)acetamide (5), achieved in three synthetic steps starting from the commercially available chemical, aniline. The chemical structure of the target OSe compound 5 was characterised using NMR, IR, and mass spectrometry. The DFT calculations were performed. The results reveal that compound 1 demonstrates the lowest HOMO energy (-5.03 eV) and the most significant energy gap (3.62 eV), indicating high stability and low reactivity. In contrast, compound 2 shows the highest HOMO energy (-3.62 eV) and the smallest energy gap (1.31 eV), confirming its high reactivity and low stability. HB168 and compound 3 demonstrate intermediate properties with moderate reactivity and stability. The Dipole Moment analysis highlights strong polarity in HB168 (6.47 Debye) and weak polarity in S2 (0.27 Debye). Additionally, compound 1 displays the highest electronegativity (3.22 eV) and lowest electrophilicity index (2.86 eV), further supporting its stability and low reactivity. Conversely, compound 2 exhibits the highest electrophilicity index (6.71 eV), indicating a strong electrophilic character. The prepared OSe compound was docked against three bacterial strain protein targets: *Escherichia coli* (ID: 5L3J) as *Gram-negative* bacteria, whereas *Bacillus subtilis* (ID: 7S3L) and *Staphylococcus aureus* (ID: 3BL6) was chosen as the *Gram-positive* bacteria. Also, molecular docking were performed against three drugs as a reference drug Ampicillin as a wide spectrum antibiotic and Ebselen, Diphenyl diselenide as a Selenium containing drugs.

Keywords: Schiff bases, Organoselenium, Anticancer, Antimicrobial, Antioxidant,

INTRODUCTION

Organoselenium (OSe) agents have earned increased concern during the decade owing to their significant medical and synthetic applications[1,2]. OSe candidates surpass oxygen and sulfur (S) in pharmaceutical properties and have outstanding activities, including antitumor and anti-inflammatory activities[3,4]. Selenorganic compounds are known for their redox-modulating activities and exhibit increased

sensitivity and selectivity in tumour cells.[5,6] Integrating the selenium centres into the backbones of organic compounds leads to new scaffolds with unprecedented therapeutic and physicochemical properties.[7]

Significant progress has been observed in preparing OSe compound as pharmaceutical agents for the past twenty years[2,4,6,8]. Several *in vivo* studies showed that OSe compound have improved bioactivity compared to their organosulfur counterparts because of their elevated amphiphilicity and pharmacokinetics[9]. Consequently, medicinal chemists often replace the S atom within the structure of natural products or bioactive compounds with selenium (Se) atoms to enhance their overall pharmaceutical profiles as well as for late-stage functionalization[10,11]. Moreover, several OSe agents have shown promising antimicrobial and antitumor properties due to their efficiency in stopping the growth of cancer cells[12].

Moreover, Se-containing compounds are known to mimic glutathione peroxidase (GPx), an enzyme that plays a crucial role in reducing oxidative stress in cells[13,14]. This property makes Se compounds particularly valuable in the treatment of diseases associated with oxidative stress, such as microbial induced diseases as well as cardiovascular diseases and neurodegenerative disorders[14,15]. For instance, diphenyl diselenide I exhibited antinociceptive, anti-inflammatory, and antioxidant activities (Fig. 1)[16,17]. Moreover, ebselen II and ethaselen III are presently explored in clinical phases as antineoplastic drugs (Figure 1)[18].

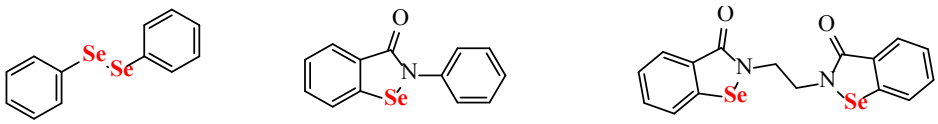

I II III

Fig. 1. Medicinally relevant organoselenium compounds

MATERIAL AND METHODS

Chemistry

OSe candidates 2-4 were synthesized according to our reported methods, starting from aniline[11,17]. See supporting information for the synthetic procedures, spectral details, and copies of the spectral analysis.

Synthesis of the target OSe N-phenyl-2-((4-(3-phenylthioureido)phenyl)selanyl) acetamide (5)

A solution of compound 4 (1206 mg, 3.96 mmol) and PhNCS (469 µL, 3.96 mmol) in CH_3OH (20 mL) was refluxed for three hours. The resulting solid formed while hot was collected and washed with CH_3OH. TLC: n-C_6H_{14} /EtOAc (4:1)]; R_f = 0.77; off-white powder; yield = 222.5 mg (42%); m.p. = 193-194°C; FT-IR (ν, cm^{-1}): 3346, 3241, 1649, 1599, 1585, 1526, 1440, 1393, 1313; ^{13}C NMR (101 MHz, pyridine-d6) δ 182.93, 170.15, 141.51, 141.44, 135.48, 130.53, 127.55, 126.84, 126.74, 126.30, 125.27, 121.48, 33.07; MS (ESI): m/z = found 405.7 [M^+-H_2S]; calcd. 440.4 [M^+].

DFT studies

For full details see the Supporting Information.

Molecular docking

The prepared OSe compound and reference drugs were docked using the Molecular Operating Environment software (MOE 2019.0102) with the protein receptors (ID: 5L3J), which refer to *Escherichia coli* DNA gyrase (ID: 3BL6), which refer to *Staphylococcus aureus* and (ID: 7S3L) which express to *Bacillus subtilis* DNA gyrase. Protein files were obtained from the Protein Data Bank as PDB files. Active pocket sites were determined in the protein using a site finder. All uncoordinated water molecules surrounding proteins were eliminated to facilitate the molecule's docking into the receptor's active pocket. The docking score was determined based on H-acceptor, H-donor bonding and/or Arene-H interactions between active sites in the proteins and the prepared compounds.

RESULTS AND DISCUSSION

Chemistry

The OSe target compound N-phenyl-2-((4-(3-phenylthioureido)phenyl)selanyl)acetamide (5) was synthesized as shown in Scheme 1 in three steps. The preparation protocol starts with the preparation of 4-selenocyanatoaniline (2) from aniline by the reaction with $CN(Se)_3CN$, produced in situ from SeO_2 and $CH_2(CN)_2$, using DMSO as the solvent. The treatment of selenocyanate 2 with an ethanolic solution of NaOH furnished the respective diselenide 3 with a good yield (88%). The treatment

of an ethanolic solution of diselenide 3 with $NaBH_4$ and subsequent reaction with $C_6H_5NHCOCH_2Cl$ led to the formation of OSe 4 in excellent yield (94%). The target compound 5 was obtained in moderate yield (42 %) through the reaction of OSe 4 with thiourea in ethanol.

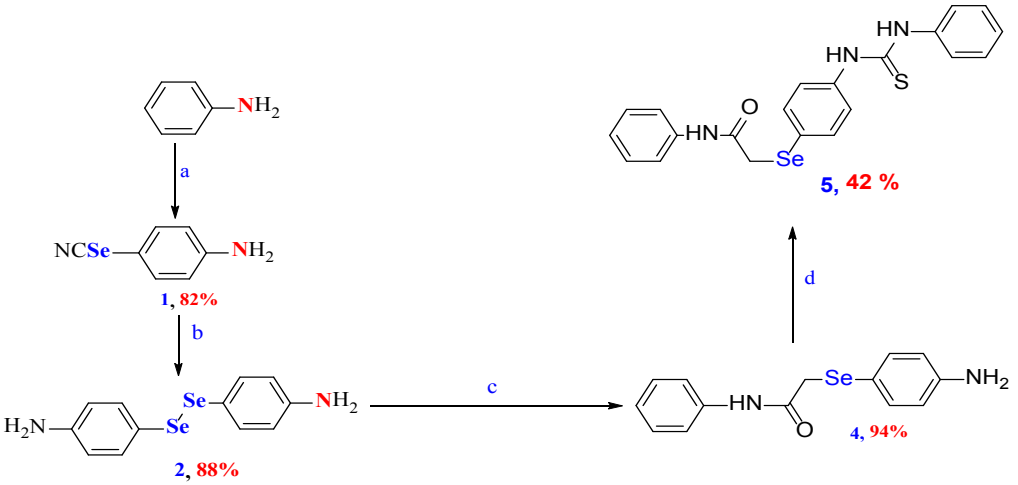

Scheme 1. The synthesis of N-phenyl-2-((4-(3-phenylthioureido)phenyl)selanyl) acetamide (5). Reagents and conditions: (a) SeO_2, $CH_2(CN)_2$, DMSO; (b) NaOH, EtOH, 3 h; (c) $PhNHCOCH_2Cl$, $NaBH_4$, NaOH, EtOH; (d) PhN=C=S, EtOH, reflux

The FT-IR spectrum of OSe 5 (Fig. SI 1) showed a characteristic peak at 3346 and 3241 cm^{-1}, which correspond to N-H stretching vibrations of the amide and thiourea. Furthermore, the C=O stretching vibration of the amide group was observed at 1649 cm^{-1}. Moreover, the C=C aromatic ring stretching vibrations were found at 1599 cm^{-1}, 1585 cm^{-1}, and 1526 cm^{-1}. On the other hand, the ^{13}CNMR spectrum 5 (Fig. SI 2) showed a deshielded signal at δ 182.93 ppm corresponding to the C=S and at δ170.15 ppm corresponding to the C=O. The aromatic carbons of the phenyl rings appeared around δ 141.51-121.48 ppm. Finally, the CHδadjacent to the Se atom was found upfield at δ 33.07 ppm.

DFT studies

Figure 1 illustrates the optimized molecular structures of compounds 2, 3, 4, and 5. These parameters provide critical insights into the molecules' stability, reactivity, and chemical behaviour, which are listed in Table 1.

Table 1: E_{HOMO}, E_{LUMO}, and molecular descriptors of compounds 2, 3, 4, and 5

Molecule	E_{HOMO}(eV)	E_{HOMO}(eV)	ΔE(eV)	η(eV)	Dipole Moment	S(eV)	χ (eV)	μ(eV)	ω(eV)
2	-5.03	-1.41	3.62	1.81	5.96	0.28	3.22	-3.22	2.86
3	-3.62	-2.31	1.31	0.66	0.27	0.76	2.97	-2.97	6.71
4	-4.3	-1.55	2.75	1.38	1.63	0.36	2.93	-2.93	3.11
5	-4.2	-2.18	2.02	1.01	6.47	0.50	3.19	-3.19	5.04

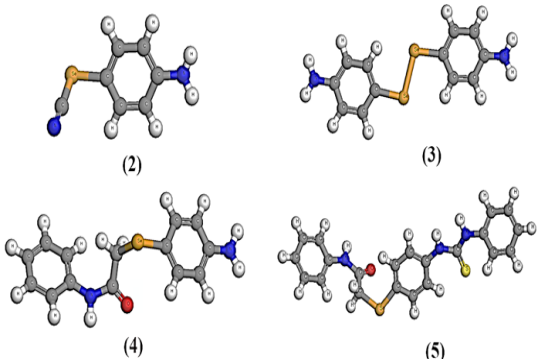

Fig. 1. Optimizes structures of the compounds 2-5

The elevated energy levels of the HOMO indicate that the molecule is effective electron donor (π donor), while the reduced energy levels of the LUMO suggest that the molecule has weaker electron-accepting ability (π acceptor). In our study, Compound 2 exhibits the lowest HOMO energy (-5.03 eV) Fig. 2, suggesting it is the most stable and least reactive among the molecules. In contrast, 3 has the highest HOMO energy (-3.62 eV), indicating it is the least stable and most reactive. The LUMO energy of Compound 2 (-1.41 eV) is also the lowest, making it a strong electron acceptor, while Compound 3 has relatively higher

LUMO energy (-2.31 eV), indicating weaker electron-accepting ability. These results are consistent with the principles of molecular orbital theory, which state that molecules with lower HOMO and LUMO energies are generally more stable and less reactive[19]

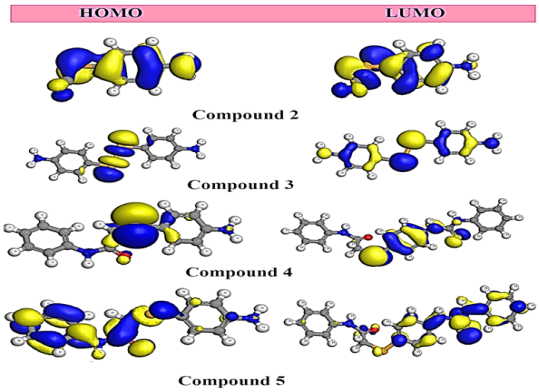

Fig. 2. 3D plots frontier orbital energies compounds 2-5

A smaller energy gap corresponds to higher reactivity and lower stability. In this study, 3 has the smallest energy gap (1.31 eV), confirming its high reactivity and low stability. On the other hand, 2 has the largest energy gap (3.62 eV), indicating it is the least reactive and most stable. Compounds 5 and 4 exhibit intermediate energy gaps (2.02 eV and 2.75 eV, respectively), suggesting moderate reactivity and stability. These findings align with the concept that a smaller energy gap facilitates easier electron excitation, leading to higher reactivity[20].

Compound 2 has the highest hardness value (1.81 eV), confirming its high stability and low reactivity. In contrast, 3 has the lowest hardness (0.66 eV) and the highest softness (0.76 eV), indicating it is the most reactive and least stable. Compounds 5 and 4 exhibit intermediate hardness and softness values, reflecting moderate reactivity and stability. These results are consistent with Pearson's hard-soft acid-base (HSAB) principle, which states that hard molecules are generally more stable and less reactive than soft molecules. Compound 5 has the highest dipole moment (6.47 Debye), indicating strong polarity and intermolecular interactions. In contrast, Compound 3 has the lowest dipole moment (0.27 Debye), suggesting weak polarity and interactions. The dipole moments of Compound 2 (5.96 Debye) and 4 (1.63 Debye) fall between these extremes, indicating moderate polarity. These results emphasize the significance of dipole moments in governing the strength of intermolecular interactions, which, in turn, can impact the physical and chemical characteristics of molecules.

Compound 2 has the highest electronegativity (3.22 eV) and the lowest chemical potential (-3.22 eV), indicating strong electron-attracting ability and high stability. In contrast, Compound 3 has the lowest electronegativity (2.97 eV) and a higher chemical potential (-2.97 eV), indicating weaker electron-attracting ability and lower stability. These results are consistent with conceptual density functional theory principles, which relate electronegativity and chemical potential to a molecule's reactivity and stability.

Compound 3 has the highest electrophilicity index (6.71 eV), indicating strong electrophilic character and high reactivity. In contrast, Compound 2 has the lowest electrophilicity index (2.86 eV), indicating weak electrophilic character and low reactivity. Compounds 4 and 5 exhibit intermediate electrophilicity values (5.04 eV and 3.11 eV, respectively), reflecting their moderate electrophilic character. These findings are consistent with the concept that molecules with higher electrophilicity indices are more reactive and less stable[21].

Molecular docking

The molecular docking study demonstrates the possibility of an effective hydrogen bond interaction between the prepared compounds and the target protein. The compounds (2-5) and reference drugs (Ampicillin, Ebselen and Diphenyl diselenide) were docked with *Escherichia coli* (ID: 5L3J), *Staphylococcus aureus* (ID: 3BL6) and *Bacillus subtilis* (ID: 7S3L) receptors. Additionally, the 2D and 3D visualizations of this interaction are displayed in Fig. 3–9 and detailed in Tables 2[22].

Our docking models suggest that the inhibitor compounds will have a strong interaction with certain proteins linked to their active sites. The data obtained reveals the most optimal conformations of the compounds along with their binding energy ratings. It also includes a comprehensive list of all hydrogen bonds present between the investigated substances and proteins.

Selenium compounds are of great importance in the pharmaceutical industry as they are used in the production of many medications that treat various diseases like Meniere's Disease, Type 2 Diabetes Mellitus, and Type 1 Diabetes Mellitus.

Molecular docking analysis indicated that the docking strength is correlated with the negativity of the docking score. Compound 5 exhibited stronger binding at the active sites of *Escherichia coli* (ID: 5L3J), *Staphylococcus aureus* (ID: 3BL6), and *Bacillus subtilis* (ID:7S3L), with more negative free binding energy scores of -7.0208 kcal/mol, -7.5712 kcal/mol, and -8.1148 kcal/mol, respectively. These values were lower than those observed for compounds 2–4 (Fig. 3–9), indicating a stronger interaction.

The molecular docking revealed that the strength of docking based on more negativity of docking score for compound 5 with *Escherichia coli* (ID:5L3J), *Staphylococcus aureus* (ID:3BL6) and *Bacillus subtilis* (ID:7S3L) active sites had a higher negative score of free binding energy (-7.0208 kcal/mol, -7.5712 kcal/mol and -8.1148 kcal/mol), respectively than score with compounds 2–4 (Figures 3–9).

Compounds 2-4 have a better docking score with *Staphylococcus aureus* (ID:3BL6) than *Staphylococcus aureus* (ID:3BL6) and *Bacillus subtilis* (ID:7S3L) as free binding energy was found to be -5.2841, -6.2533 and -6.7267 kcal/mol, respectively mainly through the interaction of Se atom with bacterial protein active sites[23]. For Compound 5 interaction with *Bacillus subtilis* (ID:7S3L), active sites with free binding energy -8.1148 kcal/mol have the best docking score through hydrogen bond interaction of -NH group with TRP77 and benzene ring with PRO58.

Molecular docking data of compounds 2- 4 showed good docking score compared with reference drugs (Ampicillin, Ebselen and Diphenyl diselenide) (Fig. 7–9) which refer to the value of the prepared compounds especially compound 5 and the future prospects involve conducting more practical studies on these compounds to maximize their potential benefits in the pharmaceutical industry In conclusion, a more negative binding energy value indicates stronger and more efficient binding. Therefore, the interaction between compound 5 and the active site receptors of *Escherichia coli* (ID: 5L3J), *Staphylococcus aureus* (ID: 3BL6), and *Bacillus subtilis* (ID: 7S3L) suggests its potential as an effective antibiotic candidate.

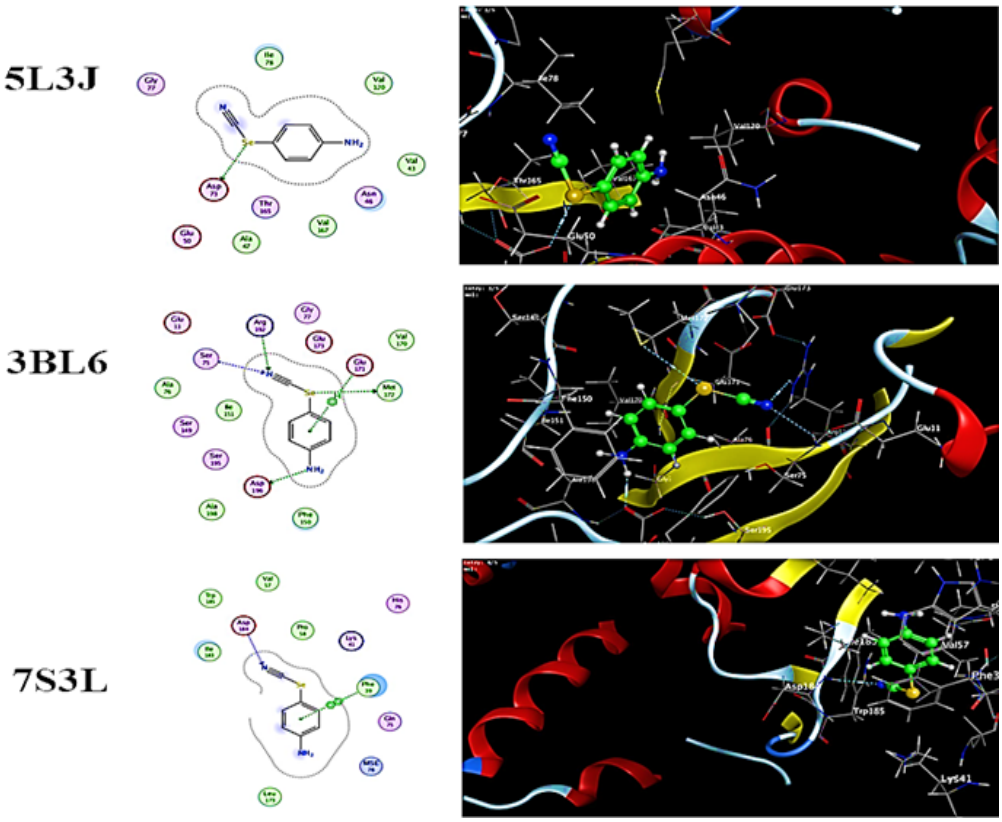

Fig. 3. 2D & 3D molecular docking interaction between compound 2 and different proteins

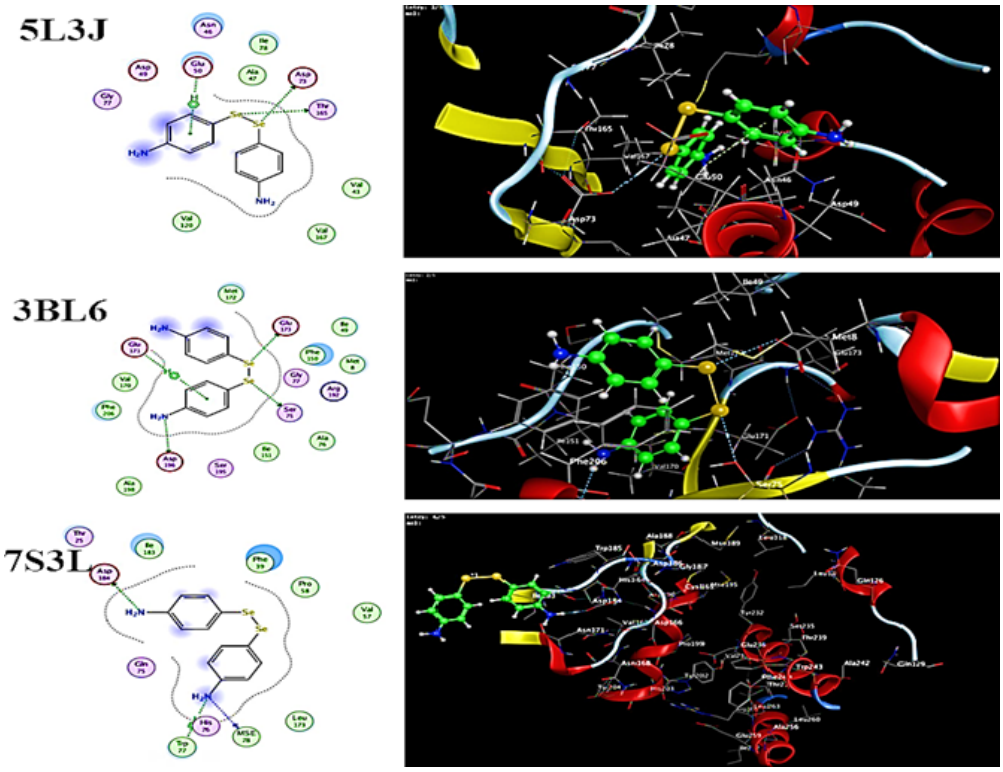

Fig. 4. 2D & 3D molecular docking interaction between compound 3 and different proteins

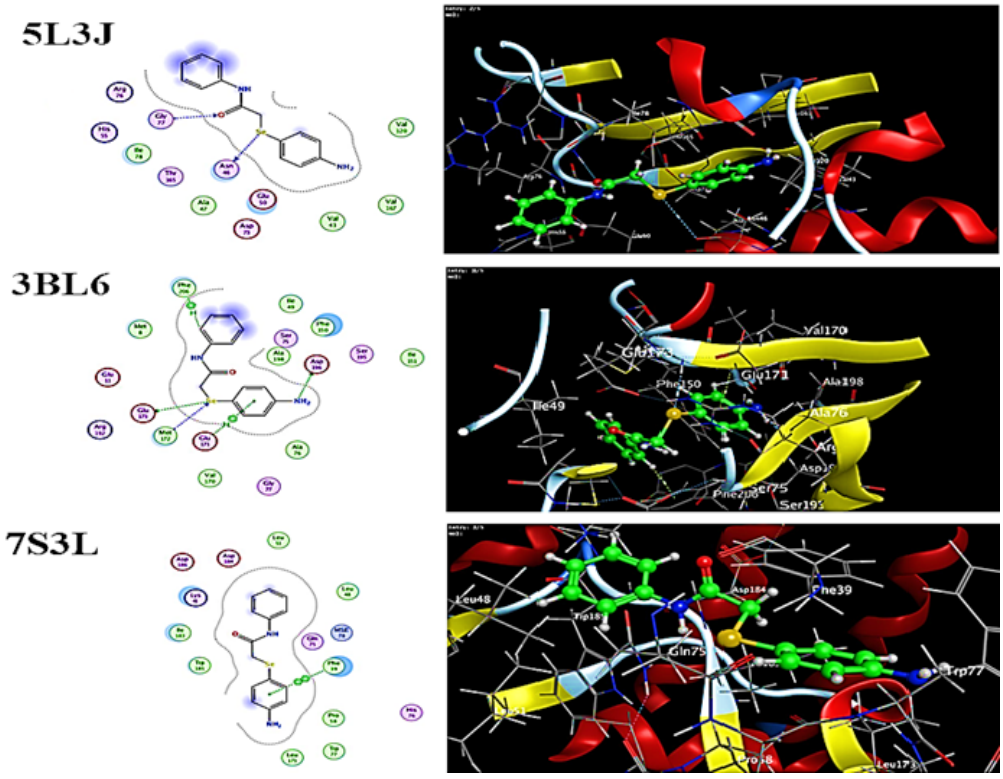

Fig. 5. 2D & 3D molecular docking interaction between compound 4 and different proteins

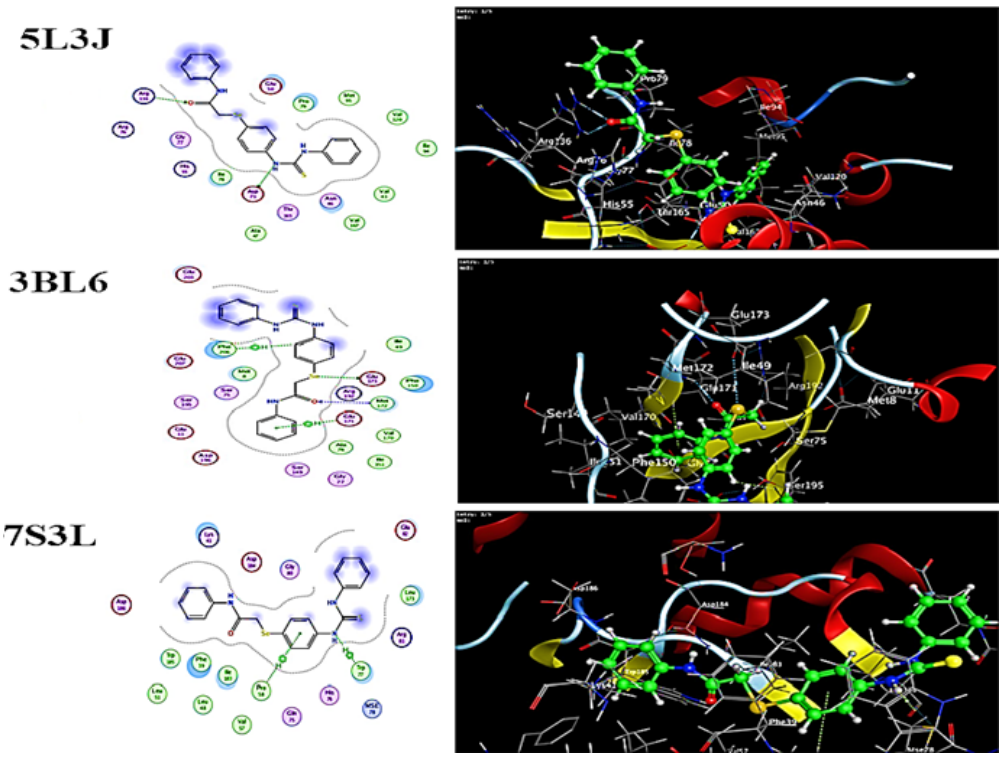

Fig. 6. 2D & 3D molecular docking interaction between compound 5 and different proteins

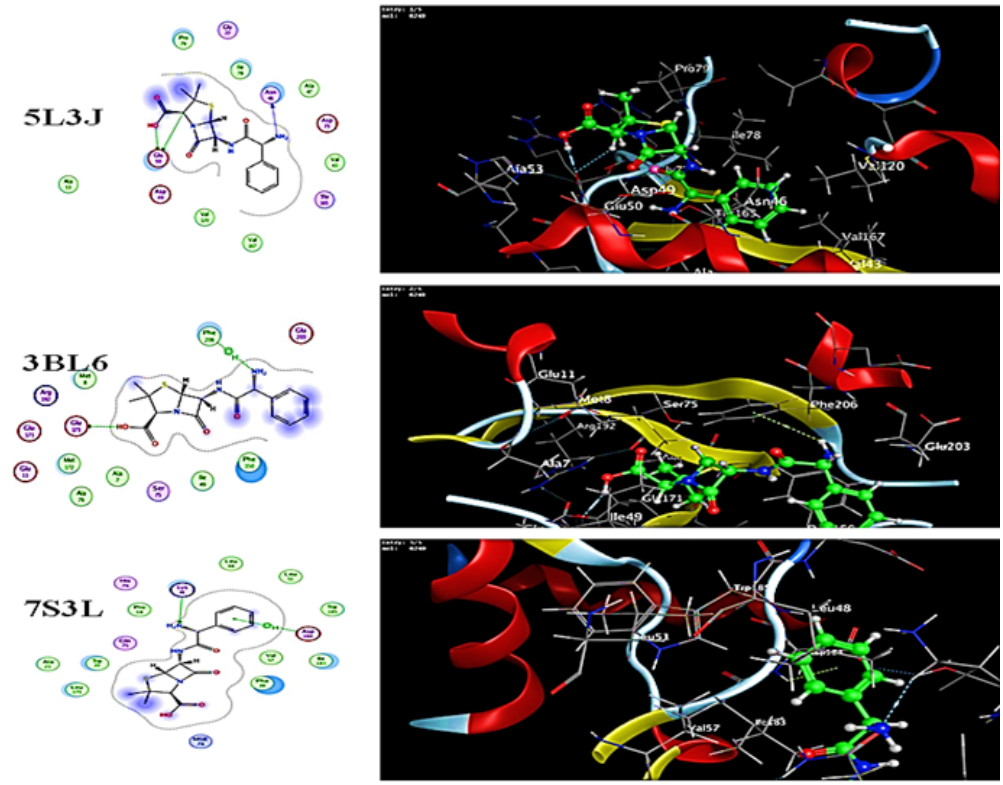

Fig. 7. 2D & 3D molecular docking interaction between Ampicillin and different proteins

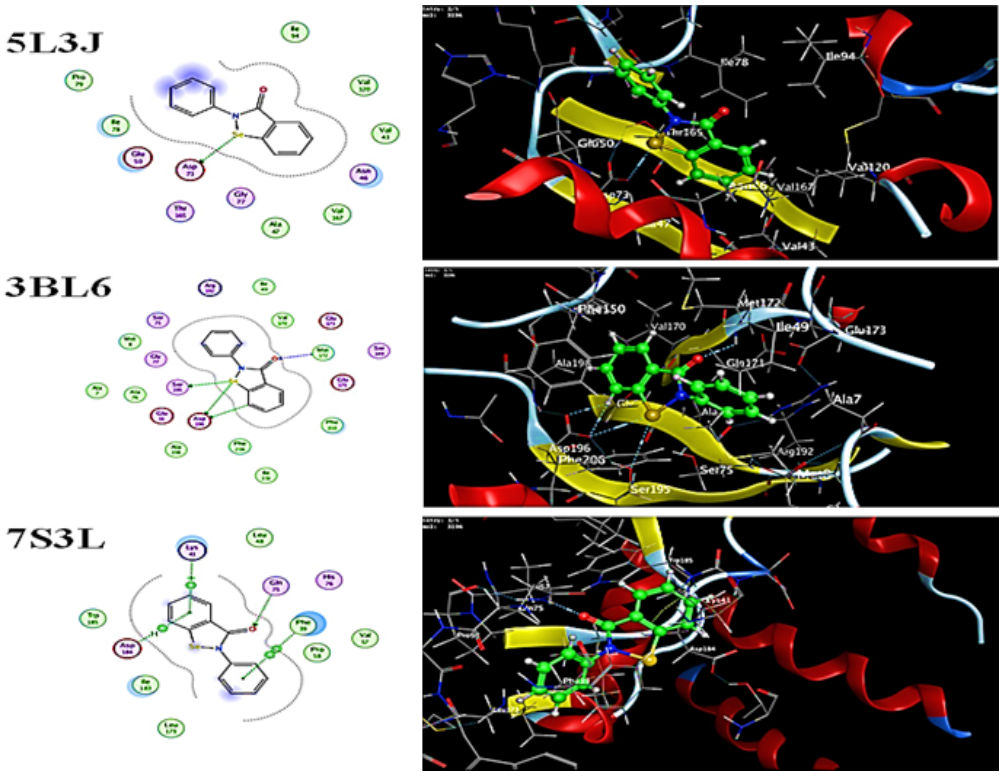

Fig. 8. 2D & 3D molecular docking interaction between Ebselen and different proteins

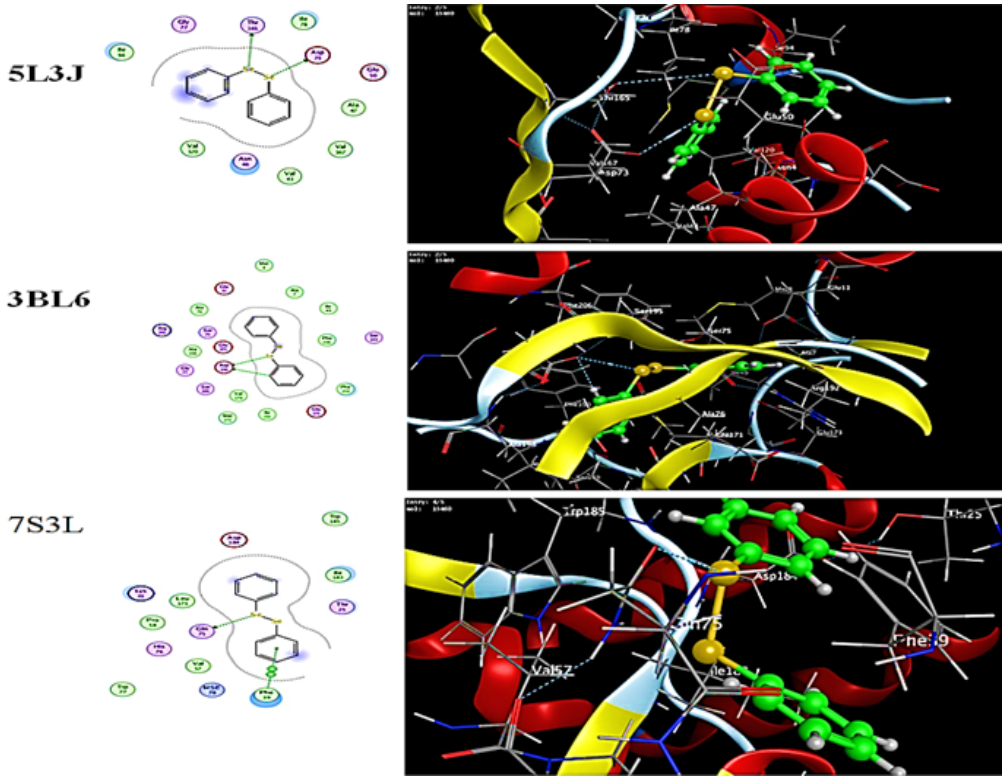

Fig. 9. 2D & 3D molecular docking interaction between Diphenyl diselenide and different proteins

Table 2: Docking scores of compounds 2-5, and standard compounds and type of bond interactions

Compound	PDB code	Bonds	interaction	Rmsd	S(kcal/mol)
Compound 2	5L3J	Se-Asp73	Sidechain donor	1.2637	-5.1089
	3bl6	Se-Met172	Sidechain acceptor	0.8688	-5.2841
		Benzene ring-Glu171	Arene-H		
		NH_2-Asp196	Sidechain donor		
		N-Ser75	Backbone acceptor		
		N-Arg192	Sidechain acceptor		
	7S3L	N-Asp184	Backbone acceptor	0.9115	-4.8493
		benzene ring-Phe39	Arene-arene		
Compound 3	5L3J	Se-The165	Sidechain acceptor	1.0672	-5.8812
		Se-Asp73	Sidechain acceptor		
		Benzene ring-Glu50	Arene-H		
	3bl6	Se-Ser75	Sidechain donor	1.5150	-6.2533
		Se-Glu173	Sidechain donor		
		N-Asp196	Sidechain donor		
		Benzene ring-Glu171	Arene-H		
	7S3L	N-Asp184	Sidechain donor	1.0621	-6.1445
		N-MSE78	Backbone donor		
		N-Trp77	H-arene		
Compound 4	5L3J	O-Gly77	Backbone acceptor	1.4598	-6.0183
		Se-Asn46	Backbone donor		
	3bl6	N-Asp196	Sidechain donor	1.9513	-6.7267
		Se-Met172	Backbone donor		
		Se-Glu173	Sidechain donor		
		Benzene ring-Glu171	Arene-H		
		C-Phe206	H-arene		
	7S3L	Benzene ring-Phe39	Arene-arene	1.6655	-6.6961
Compound 5	5L3J	O-Arg136	Sidechain acceptor	1.6497	-7.0208
		NH-Asp73	Sidechain donor		
	3bl6	O-Met172	Backbone acceptor	1.6838	-7.5712
		Se-Glu173	Sidechain donor		
		C-Phe206	Arene-H		
		Benzene ring-Glu171	Arene-H		
	7S3L	Benzene ring-Pro58	Arene-H	1.0830	-8.1448
		NH-Trp77	Arene-H		
Ampicillin	5L3J	O-Glu50	Sidechain donor	1.9153	-6.5366
		C-Glu50	Sidechain donor		
		N-Asn46	Backbone donor		
	3BL6	N-Phe206	Arene-H	1.7975	-6.2306
		O-Glu173	Sidechain donor		
	7S3L	Benzene ring-Asp184	Arene-H	1.6578	-6.2019
		N-Lys41	Sidechain acceptor		
Ebselen	5L3J	Se-Asn46	Sidechain donor	0.7801	-5.6713
	3BL6	O-Met172	Backbone acceptor	1.0097	-5.3465
		Se-Ser195	Sidechain donor		
		Se-Asp196	Sidechain donor		
		C-Asp196	Sidechain donor		
	7S3L	Benzene ring-Lys41	Arene-Cation	1.6388	-6.1699
		Benzene ring-Asp184	Arene-H		
		Benzene ring-Phe39	Arene-Arene		
		O-Gln75	Sidechain acceptor		
Diphenyl diselenide	5L3J	Se-Asp73	Sidechain donor	1.9490	-5.7775
		Se-Thr165	Sidechain donor		
	3BL6	Se-Asp196	Sidechain donor	1.5083	-5.4650
		C-Asp196	Sidechain donor		
	7S3L	Benzene ring-Phe39	Arene-Arene	1.1386	-5.4841
		Se-Gln75	Sidechain donor		

CONCLUSION

In this manuscript, the novel OSe compound namely N-phenyl-2-((4-(3-phenylthioureido)phenyl) selanyl)acetamide (5) was synthesized in three-steps synthetic protocol starting from aniline. The structure of compound 5 was confirmed using NMR, IR, and mass spectrometry.

The results indicate notable variations in the electronic properties, reactivity, and stability of Compounds 2, 3, 4, and 5. Compound 2 is the most stable and least reactive, with a large energy gap, high hardness, and strong electron-attracting ability. In contrast, Compound 3 is the least stable and most reactive, with a small energy gap, low hardness, and strong electrophilic character. Compound 5 and 4 exhibit intermediate properties, making them moderately stable and reactive. Molecular docking studies, showed that compound 5 had significant interaction with *Bacillus subtilis* (ID: 7S3L) active protein sites which suggests the potential for using this compound in the production of antibiotics in the future.

ACKNOWLEDGMENT

The authors extend their appreciation to the Deanship of Scientific Research, Imam Mohammad Ibn Saud Islamic University (IMSIU), Saudi Arabia, for funding this research work through Grant No. (221412015).

Conflict of Interest

The authors declare no competing financial interest.

REFERENCES

1. Shaaban, S.; Abdullah, K. T.; Shalabi, K.; Yousef, T. A.; Al Duaij, O. K.; Alsulaim, G. M.; Althikrallah, H. A.; Alaasar, M.; Al‐Janabi, A. S.; Abu‐Dief, A. M. Synthesis, Structural Characterization, Anticancer, Antimicrobial, Antioxidant, and Computational Assessments of Zinc(II), Iron(II), and Copper(II) Chelates Derived From Selenated Schiff base., *Applied Organometallic Chemistry*., **2024**, e7712.
2. Shaaban, S.; Ba-Ghazal, H.; Al-Faiyz, Y. S.; Al-Karmalawy, A. A.; Amri, N.; Youssef, I. Recent advances in the synthesis of organoselenium heterocycle conjugates., *Tetrahedron*., **2024**, 133957.
3. Gallo‐Rodriguez, C.; Rodriguez, J. B. Organoselenium Compounds in Medicinal Chemistry., *ChemMedChem.,* **2024**, e202400063.
4. Shaaban, S.; El-Lateef, H. M. A.; Khalaf, M. M.; Gouda, M.; Youssef, I. One-pot multicomponent polymerization, metal-, and non-metal-catalyzed synthesis of organoselenium compounds., *Polymers.,* **2022**, *14*(11), 2208.
5. Fernandes, A. P.; Gandin, V. Selenium compounds as therapeutic agents in cancer., *Biochim Biophys Acta.,* **2015**, *1850*(8), 1642-1660. DOI: 10.1016/j.bbagen.2014.10.008.
6. Shaaban, S.; Arafat, M. A.; Hamama, W. S. Vistas in the domain of organoselenocyanates., *Arkivoc*., **2014**, *2014*(1), 470-505.
7. Gandin, V.; Khalkar, P.; Braude, J.; Fernandes, A. P. Organic selenium compounds as potential chemotherapeutic agents for improved cancer treatment., *Free Radic Biol Med*., **2018**, *127*, 80-97. DOI: 10.1016/j.freeradbiomed.2018.05.001.
8. Abd El-Lateef, H. M.; Shaaban, S.; Shalabi, K.; Khalaf, M. M. Novel organoselenium-based N-mealanilic acids as efficacious corrosion inhibitors for 6061 aluminum alloy in molar HCl: In-silico modeling, electrochemical, and surface morphology studies., *Journal of the Taiwan Institute of Chemical Engineers.,* **2022**, *133*, 104258.
9. Nogueira, C. W.; Barbosa, N. V.; Rocha, J. B. Toxicology and pharmacology of synthetic organoselenium compounds: An update., *Archives of Toxicology*., **2021**, *95*, 1179-1226.
10. Nogueira, C. W.; Rocha, J. B. Toxicology and pharmacology of selenium: emphasis on synthetic organoselenium compounds., *Archives of Toxicology*., **2011**, *85*, 1313-1359.
11. Sak, M.; Al-Faiyz, Y. S.; Elsawy, H.; Shaaban, S. Novel Organoselenium Redox Modulators with Potential Anticancer, Antimicrobial, and Antioxidant Activities., *Antioxidants (Basel)*., **2022**, *11*(7), 1231.DOI: 10.3390/antiox11071231 From NLM PubMed-not-MEDLINE.
12. Sodhi, N.; Kumar, M.; Yadav, M.; Kadian, R.; Atici, S.; Friedmann Angeli, J. P.; Singh, V. P. Glutathione Peroxidase‐Mimics Organoselenium Amines: Anti‐Ferroptotic Properties and an *In silico* Study of 15‐Lipoxygenase‐2., *Asian Journal of Organic Chemistry.,* **2025**, e202400606.

13. Ringuet, M. T.; Hunne, B.; Lenz, M.; Bravo, D. M.; Furness, J. B. Analysis of Bioavailability and Induction of Glutathione Peroxidase by Dietary Nanoelemental, Organic and Inorganic Selenium., *Nutrients.*, **2021**, *13*(4), 1073. DOI: 10.3390/nu13041073 From NLM Medline.
14. Li, B.; Li, W.; Tian, Y.; Guo, S.; Qian, L.; Xu, D.; Cao, N. Selenium-Alleviated Hepatocyte Necrosis and DNA Damage in Cyclophosphamide-Treated Geese by Mitigating Oxidative Stress., *Biol Trace Elem Res.,* **2020**, *193*(2), 508-516. DOI: 10.1007/s12011-019-01717-3 From NLM Medline.
15. Xu, J.; Gong, Y.; Sun, Y.; Cai, J.; Liu, Q.; Bao, J.; Yang, J.; Zhang, Z. Impact of Selenium Deficiency on Inflammation, Oxidative Stress, and Phagocytosis in Mouse Macrophages., *Biol Trace Elem Res.*, **2020**, *194*(1), 237-243. DOI: 10.1007/s12011-019-01775-7 From NLM Medline.
16. Sonawane, A. D.; Sonawane, R. A.; Ninomiya, M.; Koketsu, M. Diorganyl diselenides: a powerful tool for the construction of selenium containing scaffolds., *Dalton Transactions.,* **2021**, *50*(37), 12764-12790.
17. Al-Abdallah, B.; Al-Faiyz, Y. S.; Shaaban, S. Anticancer, Antimicrobial, and Antioxidant Activities of Organodiselenide-Tethered Methyl Anthranilates., *Biomolecules.*, **2022**, *12*(12), 1765.
18. Wu, W.; Yang, Z.; Xiao, X.; An, T.; Li, B.; Ouyang, J.; Li, H.; Wang, C.; Zhang, Y.; Zhang, H. A thioredoxin reductase inhibitor ethaselen induces growth inhibition and apoptosis in gastric cancer., *Journal of Cancer.*, **2020**, *11*(10), 3013.
19. Shaaban, S.; Ferjani, H.; Althagafi, I.; Yousef, T. Crystal structure, Hirshfeld surface analysis, and DFT calculations of methyl (Z)-4-((4-((4-bromobenzyl) selanyl) phenyl) amino)-4-oxobut-2-enoate., *Journal of Molecular Structure.*, **2021**, *1245*, 131072.
20. Wang, B.; Geerlings, P.; Heidar-Zadeh, F.; Ayers, P. W.; De Proft, F. Exploring Intrinsic Bond Properties with the Fukui Matrix from Conceptual Density Matrix Functional Theory., *Journal of Chemical Theory and Computation.,* **2025**.
21. Chattaraj, P. K.; Maiti, B. HSAB principle applied to the time evolution of chemical reactions., *Journal of the American Chemical Society.*, **2003**, *125*(9), 2705-2710.
22. El‐Gammal, O.; El‐Reash, G. A.; Bedier, R. Synthesis, spectroscopic, DFT, biological studies and molecular docking of oxovanadium(IV), copper(II) and iron(III) complexes of a new hydrazone derived from heterocyclic hydrazide., *Appl. Organomet. Chem.*, **2019**, *33*(10), e5141.
23. Gaffer, H. E.; Elgohary, M. R.; Etman, H. A.; Shaaban, S. Antibacterial evaluation of cotton fabrics by using novel sulfonamide reactive dyes., *Pigment & Resin Technology.*, **2017**, *46*(3), 210-217.